Atmospheric Motion Vectors from Model Simulations. Part II: Interpretation as Spatial and Vertical Averages of Wind and Role of Clouds

ANGELES HERNANDEZ-CARRASCAL AND NIELS BORMANN

European Centre for Medium-Range Weather Forecasts, Reading, United Kingdom

(Manuscript received 7 December 2012, in final form 23 August 2013)

ABSTRACT

This is the second part of a two-part paper whose main objective is to improve the characterization of atmospheric motion vectors (AMVs) and their errors to guide developments in the use of AMVs in numerical weather prediction (NWP). AMVs tend to exhibit considerable systematic and random errors. These errors can arise in the AMV derivation or the interpretation of AMVs as single-level point estimates of wind. An important difficulty in the study of AMV errors is the scarcity of collocated observations of clouds and wind. The study uses instead a simulation framework: geostationary imagery for *Meteorological Satellite-8* (*Meteosat-8*) is generated from a high-resolution simulation with the Weather Research and Forecasting regional model, and AMVs are derived from sequences of these simulated images. The NWP model provides the ''truth'' with a sophisticated description of the atmosphere. This second part focuses on alternative interpretations of AMVs. The key results are 1) that interpreting the AMVs as vertical and horizontal averages of wind can give some benefits over the traditional single-level interpretation (improvements in RMSVD of 5% for high-level AMVs and 20% for low-level AMVs) and 2) that there is evidence that AMVs are more representative of either a wind average over the model cloud layer or wind at a representative level within the cloud layer than of wind at the model cloud top or cloud base.

1. Introduction

Atmospheric motion vectors (AMVs) are estimates of atmospheric wind that are derived by tracking apparent motion across sequences of meteorological satellite images, and it is known that they tend to exhibit considerable systematic and random errors and geographically varying quality, as shown in comparisons with radiosonde or numerical weather prediction (NWP) data (e.g., Bormann et al. 2002; Cotton and Forsythe 2012). AMVs are traditionally interpreted as single-level point estimates of wind, and it is generally assumed that high-level AMVs represent best the wind at the top of the cloud layer, whereas low-level AMVs are often assigned to an estimate of the base of the cloud (Hasler et al. 1979; LeMarshall et al. 1993). It is generally accepted that an accurate estimate of the cloud-top height is essential to assign a suitable height to high-level AMVs.

This is the second paper of a two-part series of papers that summarize results from a study that used a simulation framework to improve the characterization of current AMVs and their errors to guide developments in the use of AMVs in NWP. In this type of framework, a simulation from a high-resolution model provides the ''true'' atmosphere from which sequences of satellite images are generated and then used to derive AMVs. In Bormann et al. (2014, hereinafter Part I), we introduced the simulation used in the study, analyzed the realism of the resulting simulated images, and investigated the characteristics of the derived AMVs by comparing them with the true wind from the model simulation. For the latter, we followed the traditional approach of interpreting AMVs as single-level point observations.

It has often been suggested that the traditional interpretation of AMVs as single-level point estimates of wind might be one of the causes of apparent AMV errors (Rao et al. 2002; Velden and Bedka 2009). The reason becomes apparent if we consider the process of AMV derivation. In the operational derivation of AMVs from geostationary imagery, the apparent motion of radiance or a brightness temperature pattern is tracked across images by using region-matching methods. The interval between consecutive images is currently in the range of 15–30 min, and the size of the tracer boxes used in the

Corresponding author address: Niels Bormann, ECMWF, Shinfield Park, Reading RG2 9AX, United Kingdom.
E-mail: n.bormann@ecmwf.int

DOI: 10.1175/JAMC-D-12-0337.1

tracking step is typically around 24 × 24 pixels (i.e., at least 75 km × 75 km at nadir). The tracers are either clouds, which have some vertical extent, or clear-sky features, in which case the radiances represent the contribution of a deep vertical layer. It has been suggested that, considering these aspects, it would be more appropriate to interpret AMVs as vertical, horizontal, and time-averaged estimates of wind (e.g., Rao et al. 1990; Büche et al. 2006).

The interpretation of AMVs as vertical, horizontal, and time-averaged estimates of wind could be taken into account when calculating AMV equivalents from model fields in data assimilation. The process of calculating an observation equivalent from model fields is usually referred to as the ''observation operator'' in data assimilation. A well-designed observation operator and a good knowledge of the characteristics of the observation errors are needed to make optimal use of any observation by the assimilation system. The observation operator for AMVs currently consists of interpolation of the wind field to the AMV location in time and space. To test alternative interpretations, AMVs can be compared with model equivalents that have been calculated by using observation operators that include horizontal, vertical, or temporal averaging.

A number of studies have investigated the effect of interpreting the AMVs as an average wind over a layer in the vertical dimension, by comparing the AMVs with radiosonde data (e.g., Rao et al. 2002; Velden and Bedka 2009; Weissmann et al. 2013) or short-range forecasts (e.g., Bormann et al. 2002; Forsythe et al. 2010). The layer mean is typically calculated as a weighted average, using either top-hat or Gaussian weighting functions. The layers can be positioned around the originally assigned level or with their center offset relative to the originally assigned level. In a study that was based on three radiosonde sites, using an approach in which the layer was positioned below the originally assigned pressure for high-level winds, Velden and Bedka (2009) found that the AMVs compared better to radiosondes when the radiosondes were averaged over layers of ~30–100 hPa for cloudy infrared or water-vapor winds. Also using collocated radiosonde data, Weissmann et al. (2013) investigated averaging over layers below cloud-top estimates provided by lidar observations and found improvements relative to a single-level interpretation when averaging over 100–150-hPa layers. Forsythe et al. (2010) also found some benefits from calculating AMV equivalents from short-range forecasts as averages in the vertical direction, and they argued that the depth of the layer may need to be situation dependent to achieve the full benefit.

In our simulation study, the high-resolution model provides not only the true wind field, but also a very detailed description of the entire true atmosphere on a high-resolution grid. Cloud-related variables, such as liquid-water mixing ratio or ice mixing ratio, are either part of the simulation output or can be calculated from it. This fact allows the exploration of alternative interpretations of AMVs involving, for example, the vertical location of cloud layers, and also allows one to study how specific conditions of the ambient cloud affect AMV quality. Provided the simulation is realistic, the simulation framework allows a more detailed and focused analysis than is normally possible when using real observations.

In the current study, we use the possibilities offered by the simulation framework to explore alternative interpretations of AMVs as vertical as well as spatial averages and to explore the impact of reassigning AMVs to vertical levels or layers related to the model ambient cloud layer. In particular, we revisit the traditional assumption that high-level and low-level AMVs best represent, respectively, the wind at the top and at the base of the ambient cloud layer. The structure of the paper is as follows. Section 2 describes briefly the data used in the study. Section 3 focuses on the interpretation of AMVs as horizontal and vertical averages of wind. Section 4 concentrates on AMV observation operators that include cloud variables, and section 5 concludes the paper, summarizing and pointing at directions for future work.

2. Data

In this section, we give a short description of the simulation and datasets used in the study. The reader is referred to Part I for details. The model used for the simulation is the Weather Research and Forecasting (WRF) regional model, configured to cover the entire domain of the *Meteorological Satellite-8* (*Meteosat-8*) prime disk within the latitudes 58.8°S–58.8°N. In this integration the horizontal resolution varies from 3 km at the equator to 1.7 km at the north and south boundaries, and the number of vertical levels is 52, with the model top at 28 hPa. The study period spans 24 h, starting at 0000 UTC 16 August 2006, covered by a 6–30-h forecast generated by the WRF model; further details of this simulation are also available in Otkin et al. (2009).

Spinning Enhanced Visible and Infrared Imager (SEVIRI) images from the WRF simulation output were produced every 15 min using version 9 of the Radiative Transfer for the Television and Infrared Observation Satellite Operational Vertical Sounder radiative transfer package (RTTOV; Saunders et al. 2008). AMVs were subsequently derived by the European Organisation for the Exploitation of Meteorological Satellites (EUMETSAT) from the simulated imagery, using a prototype derivation system developed in preparation for

Meteosat Third Generation imagery (Borde et al. 2011). AMVs were produced half-hourly, from triplets of images. Only cloudy AMVs derived from the 10.8-μm infrared (IR) channel and 6.2-μm water vapor (WV) channel were produced for this study.

As outlined in Part I, the simulation provides a useful dataset for the characterization of AMVs. Characteristics of the simulated images compare well to observed ones, in terms of the general distribution of brightness temperatures, the temporal variability, and the effective horizontal resolution. Nevertheless, there is an indication that the upper-level humidity is too large in the WRF data. Possibly related to this situation, the simulated AMVs are assigned too high in the atmosphere when interpreted as single-level point observations (bias in pressure of 60–75 hPa). After a global correction for this bias in the assigned pressure, the AMVs derived from the simulated imagery show characteristics that are in line with those commonly found for real AMVs, with speed biases and root-mean-square vector differences (RMSVDs) for the simulated AMVs in comparison with the model truth typically within $1\,\mathrm{m\,s^{-1}}$ of values obtained from comparisons between real AMVs and short-range forecasts. Taking into account that the comparisons of the real AMVs against short-range forecasts include a contribution from forecast errors, the results suggest that the errors in the simulated AMVs are comparable to or slightly larger than those of real AMVs. For further details the reader is referred to Part I.

3. AMVs interpreted as vertical and horizontal averages of wind

This section concentrates on the evaluation of AMVs interpreted as wind averages. We consider calculating AMV equivalents from the model data by averaging over layers in the vertical dimension as well as over neighborhoods in the horizontal plane. The approach for averaging in the vertical direction is similar to that used in Velden and Bedka (2009) or Weissmann et al. (2013) with radiosonde data. It must be emphasized that all of the AMVs in this study were derived from cloudy tracers. If tests similar to the ones presented here were applied to clear-sky AMVs, the results would presumably be very different, because radiances in clear-sky tracers represent the contribution of deeper tropospheric layers.

a. Method

For each AMV in the study set, three wind profiles were extracted from the model data: 1) u and v at the nearest grid point, 2) u and v averaged over a 30-km-radius neighborhood, and 3) u and v averaged over a 40-km-radius neighborhood. Throughout the section, the labels used to identify these profile types are NR0, NR30, and NR40, respectively. The profiles include the model levels from 1 (closest to the surface) to 45 ($\sim$80 hPa). The neighborhood radii were chosen to be consistent with typical tracer sizes for AMVs. These profiles were used for vertical averaging.

For vertical averaging, this section considers layers that are positioned relative to the pressure level assigned to the AMV (possibly subject to a pressure bias correction as discussed later). In general, given a final single-level height assignment provided in the AMV product, several options are possible to position such a layer: for instance, below the assigned pressure, or centered around it, or other variations. A physically or statistically sensible choice depends on the meaning of the pressure level assigned by the producers to each AMV (and on the accuracy of that estimate, because it may be biased). It is currently standard practice for AMV users to assume that the AMVs represent wind at the assigned pressure level, that is, that the assigned pressure level is the most representative one. In this case, averaging over a layer that is centered around the assigned level makes the most sense, if the height estimate is unbiased. If the assigned pressure level is indeed a good estimate of the cloud top, however, averaging over a layer below the assigned pressure level is more justified, because it takes into account that the cloud is located below this pressure level. When averaging over a layer that is not centered around the assigned pressure, the statistical effect of layer averaging is mixed with that of effectively reassigning the AMV to a different level, one that may be more representative than the assigned pressure level. In this case, the layer averaging may have an effect that is similar statistically to simply adjusting the height assignment. This aspect is particularly relevant in this study, given the large height bias (in the assigned pressure relative to the most representative one) that was found for the simulated AMVs in the first part of this paper.

To separate the effect of layer averaging and pressure bias correction, we take a two-step approach: first, we calculate model equivalents using a single-level approach, but for a series of globally constant pressure increments p_{inc} that are added to the assigned pressure. This approach will be labeled new_HA, and we use the nearest gridpoint profiles NR0 here. These calculations are used to determine the optimal global adjustment p_{bcor} to the pressure level assigned during the AMV derivation. This optimal adjustment may be different for the IR and WV winds. Second, we calculate a layer average that is centered around this adjusted pressure (labeled bcor_centre): if amv_pres represents the original pressure and Δp is the depth of the layer for the average, the pressure interval used for the average is

$[p_0, p_1]$ = [amv_pres + p_{bcor} − $\Delta p/2$, amv_pres + p_{bcor} + $\Delta p/2$]. This choice of layer makes the most sense statistically, given that our height adjustment removes biases relative to the most representative level.

To highlight the interplay between height reassignment and layer averaging in the presence of a large bias in the assigned pressure relative to the most representative pressure, we also consider a layer that is located just below the originally assigned AMV level in the vertical direction (labeled ''Below''); that is, the pressure interval used for the average is $[p_0, p_1]$ = [amv_pres, amv_pres + Δp]. For comparison with new_HA, note that this layer is centered around the level amv_pres + p_{inc} with $p_{inc} = \Delta p/2$.

All vertical averages were calculated using a boxcar weighting function, and they use the horizontally averaged NR30 profiles unless indicated otherwise. In some cases, the pressure interval $[p_0, p_1]$ was not fully contained in the pressure interval determined by the first and last model levels in the profile; this situation happened particularly for low-level AMVs and deep layers but also occurred for high-level AMVs. In those cases the averaging interval was reduced as needed. Note that, for a given pressure bias correction p_{bcor}, the layer used in bcor_centre with the depth $\Delta p = 2p_{bcor}$ is the same as the layer for the Below case with the same depth.

b. Results

Figures 1 and 2 show how the comparison statistics—RMSVD and speed bias (AMV speed minus model wind speed)—vary with pressure increment or layer depth for high-level WV6.2 and IR10.8 AMVs, respectively. For ease of comparison, the classification as high-level wind (i.e., with a pressure < 400 hPa) is based on the originally assigned pressure here, as is done throughout this paper. In contrast to Part I, outliers have not been removed when calculating these summary statistics for the derived AMVs, and this is the same for all summary statistics presented throughout this paper. Removal of outliers is considered to be less crucial here because we are intercomparing different interpretations of the same AMV dataset. Also, during our investigations we found that groups of outliers for certain interpretations of the AMVs can at times point to important shortcomings with the interpretation used.

We first consider the new_HA curves to obtain the optimal global pressure adjustment p_{bcor}. As expected from the results presented in Part I, there is a clear improvement from assigning the AMVs to a level lower in the atmosphere, both in terms of the RMSVD and the speed bias (see Figs. 1 and 2). The RMSVDs show a minimum for p_{inc} of ~60–80 hPa for the WV6.2 AMVs and ~100 hPa for the IR10.8 AMVs (note that the x axis in these figures shows 2 times the pressure increment, as explained in the caption). The optimal speed bias is also found for similar pressure adjustments. Other levels show similar behavior for the new_HA curves, suggesting similar values for the optimal pressure adjustment (e.g., Fig. 3). On the basis of these results, we chose a global value of $p_{bcor} = 70$ hPa for the WV6.2 AMVs and $p_{bcor} = 100$ hPa for the IR10.8 AMVs. Although the optimal p_{inc} differs slightly by geographical region, the differences in comparison with the global values are relatively minor (± 20 hPa). The values for the optimal height reassignment are slightly larger than the pressure bias corrections applied in Part I (60 and 75 hPa for WV6.2 and IR10.8 AMVs, respectively), where the adjustments were derived from best-fit pressure statistics. The differences are relatively small, however, suggesting that the best-fit pressure statistics and the approach taken here give qualitatively similar results.

We can now consider the effect of horizontal and vertical averaging. As expected, the Below curves in Figs. 1 and 2 share the general shape of the new_HA curves, both in terms of the RMSVD and the speed bias. This is because the layer Below the originally assigned pressure level implicitly also lowers the height assignment. The optimal values for the layer depth are found for a layer for which the center coincides with the optimal reassignment. This result highlights how this choice of layer averaging can show particularly strong benefits in the presence of a strong bias in the assigned pressure relative to the representative pressure. Comparison of the Below and new_HA nevertheless shows that the averaging leads to considerably lower RMSVDs on top of the benefits from the height reassignment, however.

The bcor_centre curves in Figs. 1–3 allow a better appreciation of the effect of layer averaging separated from the issue of the pressure bias. For all layers and regions considered, layer averaging around the bias-corrected pressure leads to some benefit in terms of the RMSVD. The curves exhibit a shallow minimum, located mostly around layer depths of 160–180 hPa (100–140 hPa for high-level AMVs in the tropics). The speed bias is relatively stable with layer depth for this type of vertical averaging, except for the tropics for which the bias increases with layer depth.

Horizontal averaging also improves the comparison statistics slightly. This can be seen, for instance, in Figs. 1–3: the new_HA curves are calculated using the wind profile of the WRF grid point closest to the AMV location (NR0), whereas the Below and bcor_centre curves are using an average over a neighborhood with a radius of 30 km (NR30). The difference between statistics of the new_HA curves (where there is no vertical or horizontal averaging) at the optimal pressure increment and the

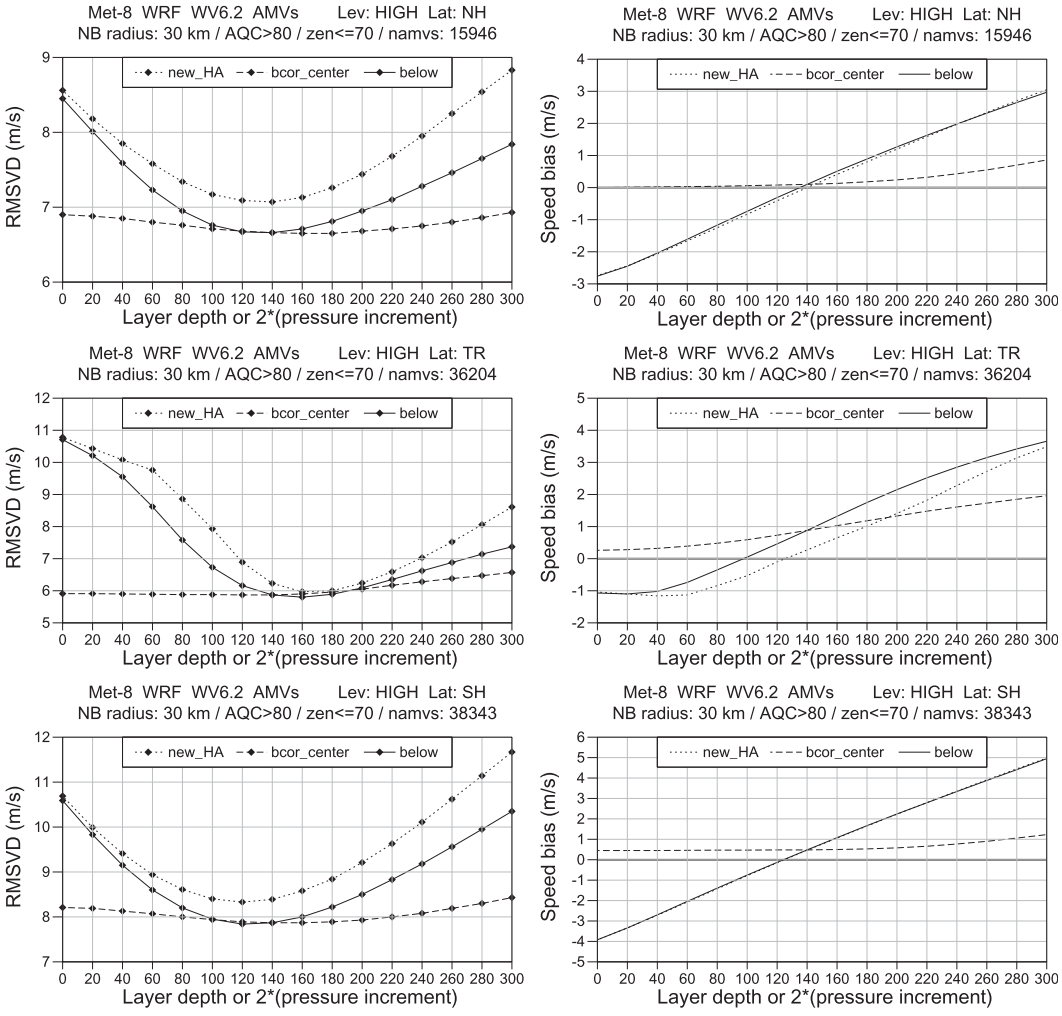

FIG. 1. (left) RMSVD and (right) bias curves, as layer depth (or pressure increment) increases, for high-level WV6.2 AMVs for the (top) Northern Hemisphere extratropics (NH), (middle) tropics (TR), and (bottom) Southern Hemisphere extratropics (SH). Curves show AMVs interpreted as vertical averages over a layer centered around the bias-corrected assigned pressure (dashed; bcor_centre), as vertical averages over a layer just below the original level (solid; Below), and evaluated after being assigned to an increased pressure (dotted; new_HA). Notice that in the last case the *x* axis shows 2 times the pressure increment whereas for the other curves it shows the layer depth. This is so that for a given layer depth the corresponding pressure increment places the wind at the center of the Below layer. In the cases of layer averaging, the model winds were also averaged horizontally over a 30-km neighborhood. Only AMVs with a model-independent QI $>$ 80% were selected.

bcor_centre curve at a layer depth of 0 hPa (where there is horizontal but no vertical averaging) suggests some benefits for the RMSVD for horizontal averaging before vertical averaging. The effect of the horizontal averaging on the Below layer can be seen more easily in Table 1. It shows the influence of using different horizontal averaging approaches on the comparison statistics for high-level WV6.2 AMVs for the 140-hPa layer depth. The layer depth of 140 hPa is the optimal layer depth for this type of winds, according to Fig. 1. Since the bias correction applied to WV6.2 AMVs is 70 hPa, the Below and bcor_centre layers coincide for this layer depth. For the three latitude bands, the RMSVD is slightly better for NR30 than for NR0 and is very similar for NR30 and NR40; a similar pattern can be noticed for other depths (not shown). The effect is fairly small, however: typically limited to an improvement of 0.1–0.3 m s^{-1}.

The combined effect of horizontal and vertical averaging for the simulated data leads to an improvement in RMSVD of up to ~5% for high-level AMVs and 20% for low-level AMVs. These findings have to be viewed in the context of the horizontal and vertical variability represented in the WRF model data. Given the nominal grid resolution (1.7–3 km), the effective resolution of the

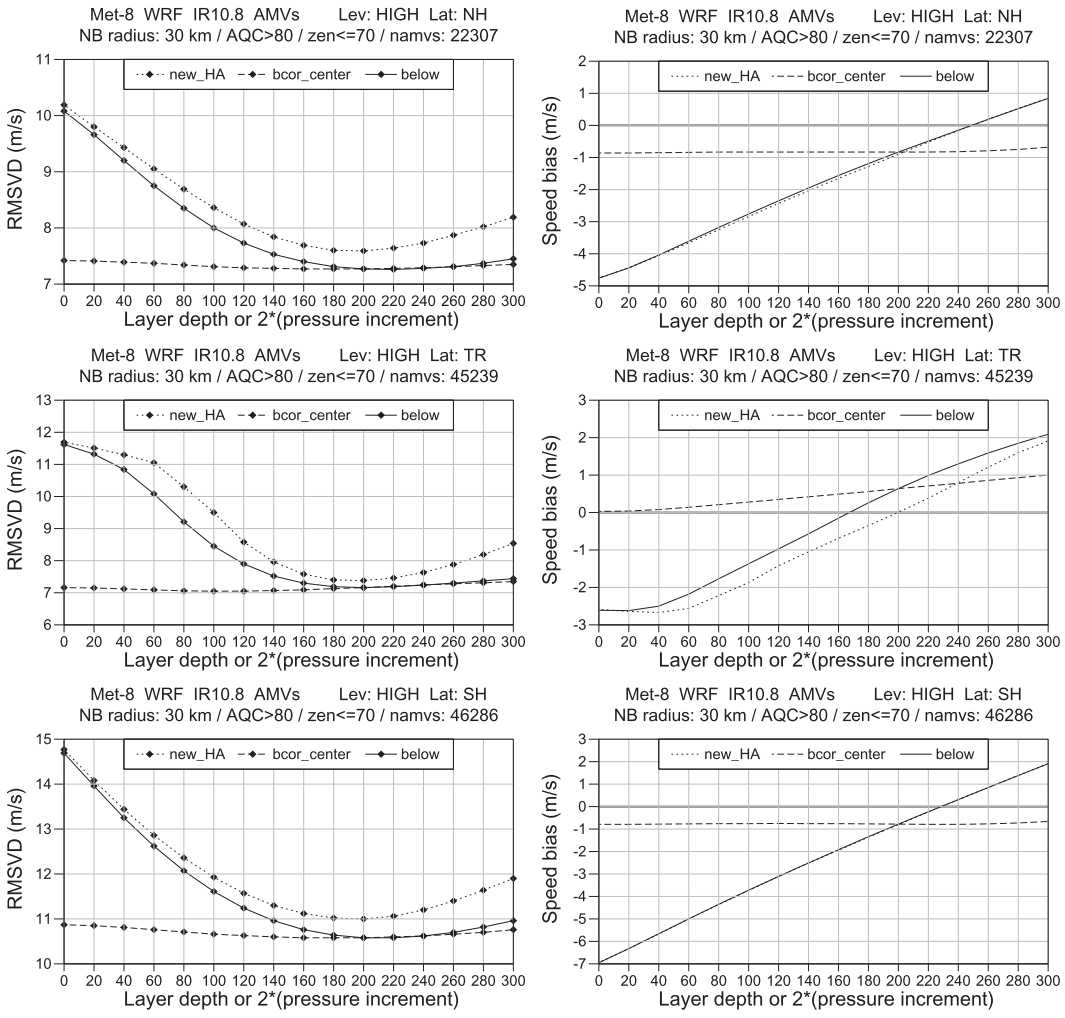

FIG. 2. As in Fig. 1, but for high-level IR10.8 AMVs.

model wind field will be lower (~10–15 km), and the inherent smooth representation means that the effect of spatial averaging of the wind field may be underestimated in our simulation framework. This also holds for the vertical representation, which is subject to the model's effective vertical resolution. For instance, when comparing AMVs with radiosondes that may capture more vertical variability, the benefit of layer averaging is likely to be higher. The scales represented in the WRF simulation are expected to be comparable to or finer than those represented in today's global NWP systems, however, and our results are hence likely to be more indicative of the magnitude of the benefit achievable from layer averaging in these systems. Note also that no attempt was made to separate results according to the local horizontal variation of wind or the variation of wind shear. For instance, the small differences between different neighborhood radii for the horizontal averaging may reflect the relative smoothness of the wind field at high levels, with notorious exceptions such as the jet. Restricting the analysis to cases of significant horizontal variation or variable wind shear would likely give better insight into the value of vertical or horizontal averaging in specific cases.

The finding that layer averaging can be beneficial when comparing AMVs with profile data is consistent with findings of previous studies (Velden and Bedka 2009; Forsythe et al. 2010; Weissmann et al. 2013). Velden and Bedka (2009) compared AMVs from National Oceanic and Atmospheric Administration/National Environmental Satellite, Data, and Information Service operations with radiosonde observations of winds at three different locations. For high-level cloudy AMVs, they found a consistent better agreement between AMVs and radiosonde winds averaged over a layer below the assigned pressure than between AMVs and the radiosonde

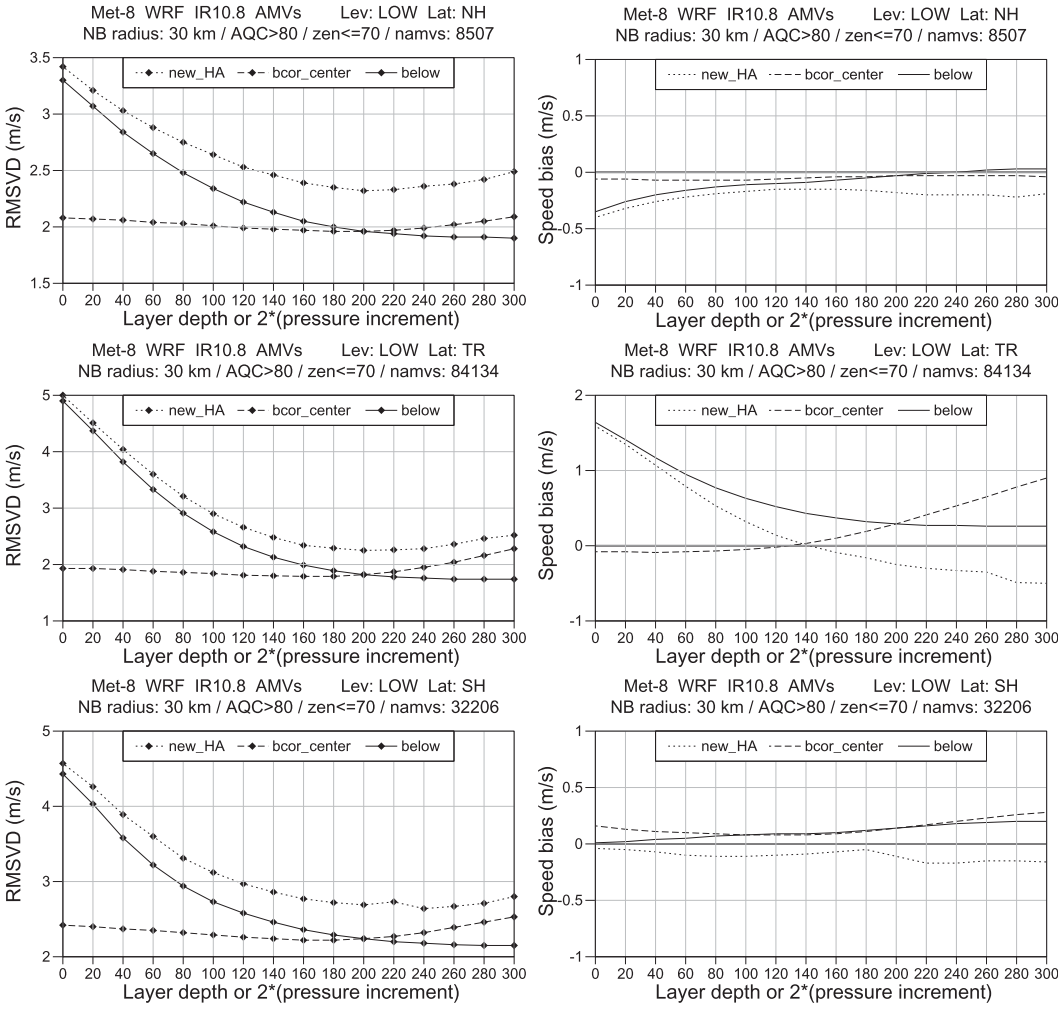

FIG. 3. As in Fig. 1, but for low-level IR10.8 AMVs. Note that for the new_HA curves AMVs located below the lowest model level after the height reassignment were omitted (roughly one-half of the number of AMVs at the largest reassignment shown), whereas for the other curves all winds were included, but the layer was restricted as described in the text.

wind at the assigned pressure (up to ~10%). Optimal depths varied between 30 and 100 hPa, depending on radiosonde site, height assignment method, vertical level, and spectral band. For a dataset over the western North Pacific Ocean, Weissmann et al. (2013) show that radiosondes averaged over layers of 100-hPa depth match AMVs better than radiosondes averaged over a 10-hPa layer, with an improvement in RMSVD of 5%–10%. They also investigated the positioning of the layer relative to the originally assigned level or relative to an accurate

TABLE 1. Summary statistics for high-level AMVs derived from WRF-simulated WV6.2 images, evaluated as horizontal and vertical averages. Only winds with a model-independent QI > 80% have been used (*Meteosat-8* WV6.2 AMVs; high level; layer: [−70, 70 hPa]; layer position: bcor_centre).

	NH			TR			SH		
	NR0	NR30	NR40	NR0	NR30	NR40	NR0	NR30	NR40
No.	16 499	16 499	16 499	36 289	36 289	36 289	39 205	39 205	39 205
Speed bias ($m\,s^{-1}$)	0.15	0.13	0.12	0.95	0.88	0.86	0.49	0.46	0.45
AMV speed ($m\,s^{-1}$)	21.25	21.25	21.25	13.80	13.80	13.80	37.81	37.81	37.81
RMSVD ($m\,s^{-1}$)	6.74	6.67	6.66	5.99	5.87	5.87	7.96	7.89	7.87
NRMSVD ($m\,s^{-1}$)	0.317	0.314	0.313	0.434	0.425	0.425	0.210	0.209	0.208

lidar-based cloud-top estimate. They concluded that a layer either centered around the assigned level or below the cloud-top estimate is best for high-level AMVs. Relative to both of these studies, our estimates of optimal layer depths are somewhat larger, most likely a result of different positioning of the layer relative to the assigned level and the use of radiosonde rather than model data. Forsythe et al. (2010) compared real AMVs from *Meteosat-9* IR10.8 imagery with first-guess observation equivalents in the Met Office system, treating AMVs as layer observations using a Gaussian weighting function rather than the boxcar function used here. They found up to a 5% reduction in mean vector difference when AMVs were interpreted as vertical averages, when compared with the traditional interpretation. They found that the best results were obtained for layers described by a Gaussian of 20–90-hPa width.

4. Observation operators that involve cloud variables

In this section we investigate different interpretations of the AMVs, taking into account the known location and characteristics of the cloud layers. This is possible in our simulation framework because the true four-dimensional distribution of the clouds is fully known. This information is used in two ways: first, to identify atmospheric situations for which the interpretation of AMVs should be simpler and, second, to aid interpretation of the AMVs themselves, for instance by attributing the AMVs to heights or layers obtained from the location of the model clouds directly. The aim is to shed light on which level or layer of the cloud is most representative of the apparent motion captured by AMVs. Information on the distribution of clouds is normally incomplete when dealing with real AMVs, and therefore such investigations are much more problematic.

a. Methods

1) CLASSIFICATION OF AMVS ACCORDING TO COLLOCATED MODEL CLOUD PROFILES

A simulation framework allows one to design model-based classifications of ambient cloud profiles. In this study we use a simple classification of AMVs, according to the characteristics of collocated model profiles, into ice/liquid and single-/multilayer cloud situations. The main purpose of this classification is to identify situations with a single cloud layer and to distinguish between ice and liquid-water cloud layers, and it has the advantage that it is based directly on model output. A more sophisticated classification that also distinguishes, for instance, convective and nonconvective cases would be possible but is beyond the scope of the current study.

TABLE 2. Cloud-profile types according to the number of ice and liquid-water cloud layers, and relative frequency (%) of each cloud-profile type for the datasets of AMVs derived from the WRF IR10.8 and WV6.2 sets of simulated images.

Label	Description	IR10.8 AMVs	WV6.2 AMVs
Clear	No cloud layers present	6.4	29.9
Ice1	One ice cloud layer	11.7	43.6
Liq1	One liquid-water cloud layer	29.9	2.2
Multilayer	Several liquid or ice cloud layers	52.0	24.3

We classify the cloud profiles into the four categories shown in Table 2. The classification considers the profiles of cloud fraction and the total mixing ratios of all liquid or ice species of the WRF model combined. These were obtained from a neighborhood with a radius of 30 km around the assigned AMV location, with the cloud fraction being the relative frequency of cloudy grid points in the neighborhood and the mixing ratios calculated as the average over the cloudy grid points. In the ideal case, this step should have taken into account the extent of the actual feature tracked in the AMV derivation. This information was not available in the AMV dataset, however, and instead a neighborhood consistent with the typical feature size was used. Note that simply using the WRF cloud information from the grid point nearest to the AMV location was found to be inappropriate in this context, because of the large spatial variability of clouds. For our classification, a model level is considered to be cloudy if more than 15% of the model grid points in the 30-km-radius neighborhood are cloudy, and the mean ice mixing ratio (respectively liquid-water mixing ratio) is above a threshold value of $10^{-4}\,\mathrm{g\,kg^{-1}}$. An ice (respectively liquid-water) cloud layer is formed by a set of consecutive ice (respectively liquid-water) cloud levels. In the classification of AMVs from the WV6.2 imagery, cloud levels below 700 hPa were ignored, as their contribution to the top-of-atmosphere radiance is negligible for this channel.

Table 2 also shows the relative frequency of each cloud-profile type, for AMVs derived from the WRF WV6.2 and WRF IR10.8 sets of simulated images. Two points are apparent: one is the high frequency of AMVs classified as clear according to the model profiles, especially in the case of the WV6.2 imagery. This is surprising, considering that the AMVs have been classified as originating from cloudy tracers. This is partly the result of a shortcoming of the cloud classification used in the AMV derivation, which also considers low-level clouds even though these are unlikely to be visible in the WV images. In addition, small differences in the

biases in the simulated dataset may also lead to misclassifications in the cloud analysis during the AMV derivation. Another striking point is the high occurrence of multilayer situations. It is generally recognized that multilayer situations are very challenging and in some cases are not handled well by current operational derivation systems, both in terms of the tracking and the height assignment; the high occurrence implies that it is potentially an important source of AMV errors. Note, however, that this classification has a tendency to overestimate the occurrence of multilayer situations. In some scenes that are multilayer from the model perspective, the contribution from lower layers to the top-of-the-atmosphere radiance is negligible; that is, the image may only represent cloud information from the top layer. In addition, cases such as one mixed ice and liquid-water cloud layer would be labeled as multilayer according to this classification. The main purpose of the classification is to identify situations for which height assignment should be less problematic.

2) MODEL WIND CALCULATIONS

In the following, we consider different interpretations of AMVs (or observation operators) and make use of the cloud information in the model data to attribute the AMV to a certain level or layer. The cloud-layer definition is as in the previous section, and the cloud top (base) is the highest (lowest) model level that is considered to be cloudy. When AMVs are interpreted as single-level point estimates of wind, the model wind is calculated by linear interpolation of the wind profile of the nearest grid point to the chosen pressure. The following interpretations are used:

1) pTop—AMVs are interpreted as single-level point estimates of wind at the top of the model cloud (note that this is the traditional view of what high-level AMVs best represent),
2) pBot—AMVs are interpreted as single-level point estimates of wind at the bottom of the model cloud (note that this is the level to which low-level AMVs are often assigned) (following Hasler et al. 1979),
3) pMean—AMVs are interpreted as single-level point estimates of wind, at a pressure within the model cloud, calculated as an average pressure over the top cloud layer, with weights proportional to the ice (or liquid water) mixing ratio (it tends to be close to the maximum of the ice or liquid water mixing ratio), and
4) VerAve—AMVs are interpreted as an average of wind over the top model cloud layer. The model wind is calculated as an average over all of the model levels from the bottom to the top of the layer, of the neighborhood-averaged profiles of u and v.

The above interpretations all depend directly on the model clouds and are independent of the height assignment provided in the AMV product. For further reference we also use the following:

1) pAmvBcor—AMVs are interpreted as single-level point estimates of wind at the bias-corrected pressure assigned to the AMV, using a pressure bias correction similar to the one introduced in Part I (following the results of the previous section, this bias correction adds 70 hPa to the originally assigned pressure for WV6.2 winds and 100 hPa for IR10.8 winds) and
2) LBF—the model wind is taken at the level of best fit (LBF) pressure, defined as the tropospheric pressure minimizing the vector difference between (u, v) from the AMV and (u, v) from the model wind profile of the nearest grid point, assuming a linear variation of u and v between model levels.

b. Results

In the following, we restrict our analysis to cases with a single cloud layer, because this simplifies the investigations into the relationship between the model cloud and the derived wind. In these cases, there is no ambiguity regarding the cloud layer used for calculating the model wind, and also the difficulties brought by multilayer situations are avoided.

1) HIGH-LEVEL AMVS

We first analyze high-level AMVs for which a single ice cloud is present. In panels a–d of Figs. 4–6 we show two-dimensional distributions of AMV and model speed and direction for the different interpretations of AMVs considered, and Table 3 provides summary statistics.

The results indicate a clear benefit from either interpreting the AMV as representing wind at a level within the cloud (pMean) or as an average wind over the cloud layer (VerAve) when compared with assigning the AMV to the top of the cloud (pTop). Assignment to the top of the cloud layer leads to marked slow biases (including in the tropics). Of interest is that the results for pTop are similar to those obtained when assigning the wind to the original pressure level provided in the simulated AMV product (not shown). In contrast, reassignment to a layer-average pressure or interpreting the AMV as an average over the cloud layer leads to a clear improvement in bias and RMSVD (Table 3) and sharper, more symmetric distributions of speed and direction (Figs. 4–6, panels c and d). The latter is particularly the case for the tropics for pMean. For the tropics, the pMean or VerAve interpretation also gives clearly better results than the interpolation to the bias-adjusted pressure level provided in the AMV product (pAmvBcor), as a result

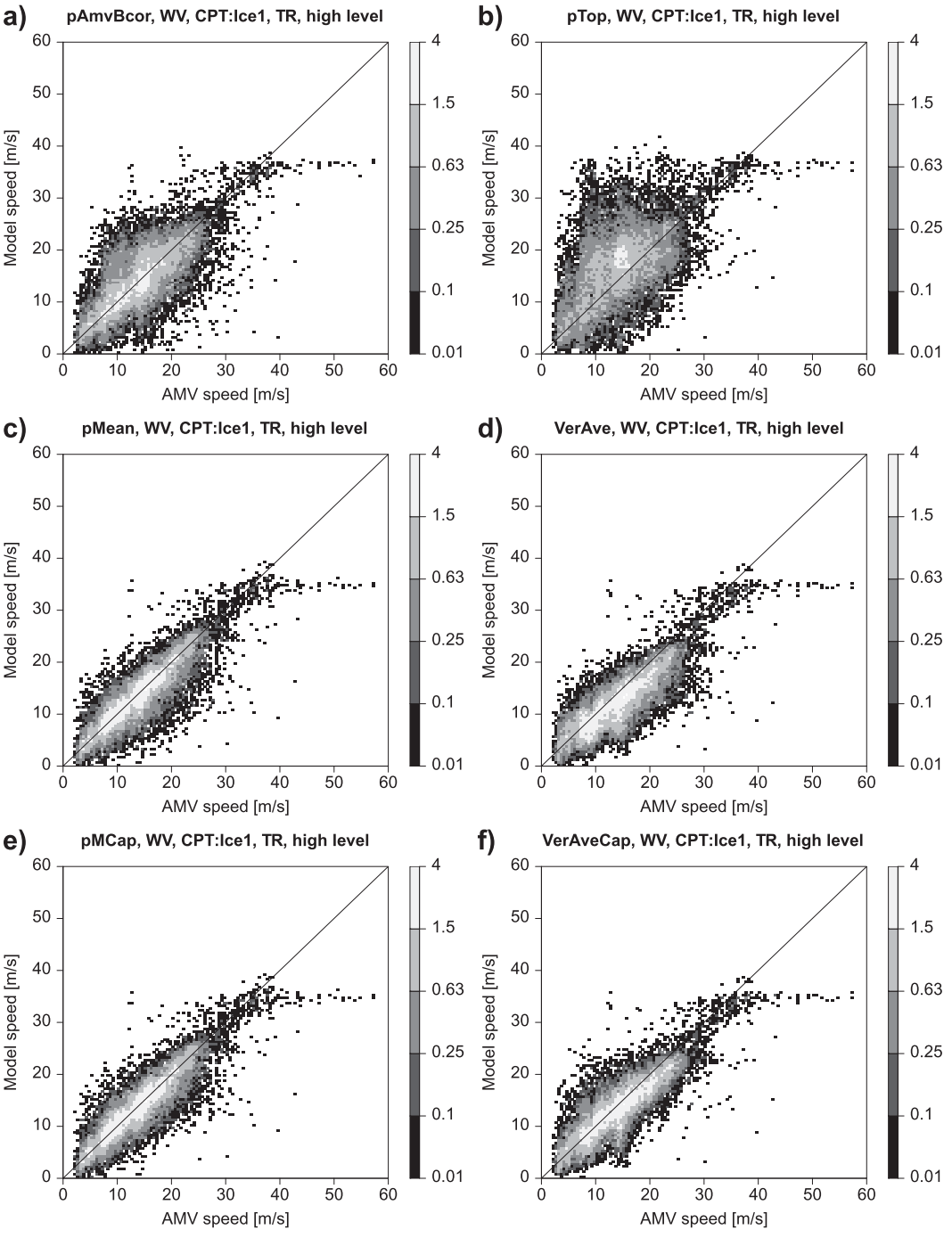

FIG. 4. Two-dimensional histograms of speed for high-level WV6.2 AMVs in the tropics for cases in which only a single ice cloud is present in the WRF data. Shown are results for the different AMV interpretations considered in this study: with the model wind linearly interpolated (a) to the bias-corrected pressure assigned to the AMV (pAmvBcor) and (b) to the top of the cloud (pTop), or (c) to an average pressure over the cloud layer (pMean) or (d) with the model wind calculated as an average of wind over the cloud layer (VerAve). Also shown are variants of pMean and VerAve for which the influence of layers or levels too far below the cloud top has been limited: (e) pMCap and (f) VerAveCap. See text for further details. Only AMVs with a model-independent QI > 80% have been selected. The shading indicates the fraction of AMVs (‰) per 0.5 m s^{-1} bin relative to the number of AMVs in the considered region.

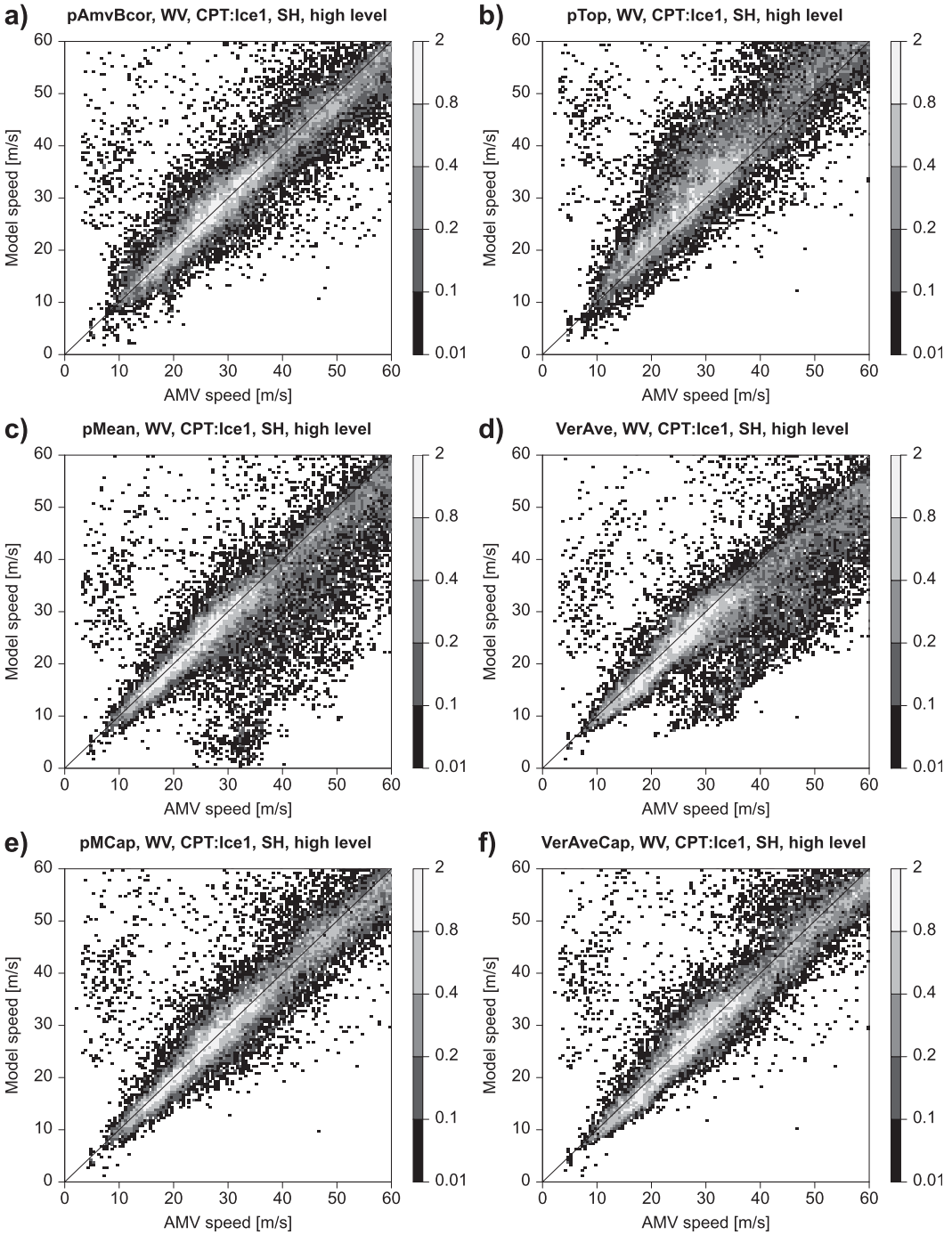

FIG. 5. As in Fig. 4, but for the Southern Hemisphere extratropics.

of using the true information on the positioning of the cloud in the vertical direction. Over the Southern Hemisphere, the agreement between AMV and model speed is also improved for pMean and VerAve when compared with pTop (Fig. 5), even though the RMSVD and speed bias shown in Table 3 do not reflect this, because of the presence of a number of outliers (e.g., around AMV speeds of $30\,\mathrm{m\,s^{-1}}$ and considerably lower model speeds in Figs. 5c and 5d). Also, pMean and VerAve show sharper distributions than pAmvBcor for lower wind speeds (up to $\sim 30\,\mathrm{m\,s^{-1}}$) but higher wind speeds exhibit larger dispersions (Fig. 5).

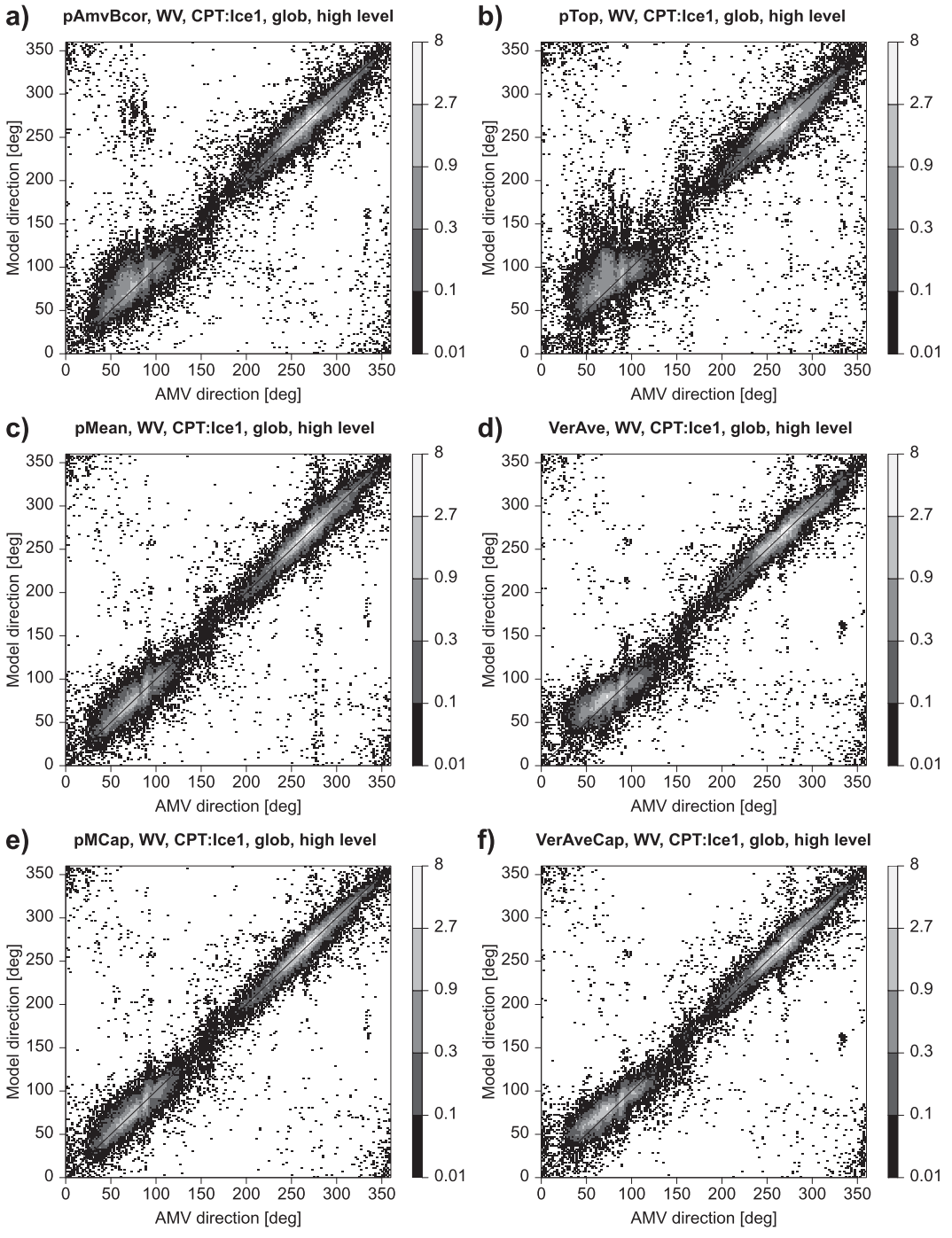

FIG. 6. As in Fig. 4, but for global two-dimensional histograms of the direction of the AMV and model wind (‰ per 2° bin). Note that the westerlies around 270° originate primarily from the extratropics, whereas the easterlies around 90° are mostly from the tropics.

Further investigations showed that the outliers for pMean or VerAve in Figs. 5c and 5d are caused by cases for which these interpretations tend to locate the AMVs too low in the vertical dimension, toward levels that are already totally obscured by the cloud in the imagery. To avoid this, we considered the following additional interpretations that restrict the influence of levels too far below the cloud top:

TABLE 3. Statistics for high-level WV6.2 AMVs with only one ice cloud layer, for different model-equivalent winds (WRF WV6.2 AMVs; high level; QI > 80%; Ice1).

		NH	TR	SH
No.		11 693	22 538	25 117
AMV speed ($m\,s^{-1}$)		21.7	14.4	36.5
Speed bias ($m\,s^{-1}$)	pAmvBcor	0.2	0.0	0.5
	pTop	−3.2	−2.4	−4.0
	pMean	−0.1	0.6	3.4
	pMCap	−0.5	0.4	0.0
	VerAve	1.1	2.0	4.5
	VerAveCap	0.1	0.8	0.2
RMSVD ($m\,s^{-1}$)	pAmvBcor	7.1	6.6	8.4
	pTop	8.7	9.2	11.6
	pMean	6.4	4.3	10.4
	pMCap	6.3	4.0	7.3
	VerAve	6.6	5.1	10.2
	VerAveCap	6.2	4.4	7.4

1) pMCap—this case is a variant of pMean in which the model wind is obtained by linear interpolation of the wind profile at the nearest grid point to the pressure pMCap = min(pMean, pTop + cap) and
2) VerAveCap— this case, in a similar way, is a variant of VerAve in which the bottom of the layer is set to min(pBot, pTop + cap).

A value of cap = 100 hPa for pMCap gave the best results overall, whereas for VerAveCap a value of cap = 180 hPa for the extratropics and cap = 120 hPa for the tropics performed best, and these values are used here. The best choice for each individual AMV is likely to depend on the cloud optical depth and is hence likely to be situation dependent. The results for pMCap and VerAveCap are shown in the bottom row in Figs. 4–6 and Table 3. A comparison to the results for pMean and VerAve shows that the number of outliers decreases considerably and also that the larger dispersion at high wind speeds is reduced markedly. This also results in a clear improvement in both RMSVD and bias (Table 3)—particularly noticeable in the Southern Hemisphere (the winter hemisphere in the study).

The influence of the thickness of the cloud layer is further investigated in Fig. 7, which shows how average RMSVD and speed bias vary with the depth of the cloud layer for the pMean model equivalent, for WV6.2 AMVs in the Ice1 class. Similar curves are also shown for the LBF, as reference. Note that the LBF RMSVD curve serves as a lower bound, because by definition the LBF represents the best possible RMSVD value. There is a clear increase in RMSVD from around 180 hPa for the pMean. The LBF RMSVD is remarkably stable, however, if we leave aside bins with very few data, which supports the view that the deterioration of the pMean

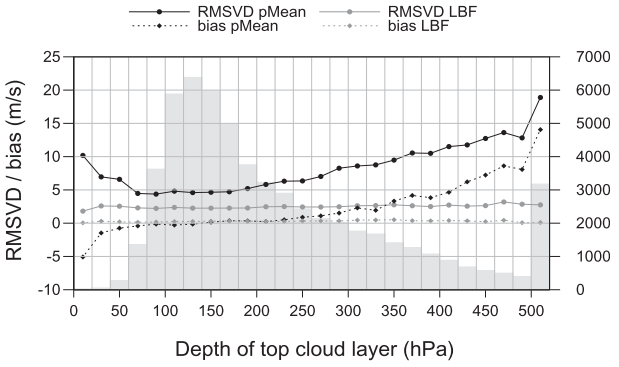

FIG. 7. RMSVD and bias curves as a function of cloud-layer depth for the pMean model equivalent (black lines) for high-level WV6.2 AMVs in the Ice1 class with a model-independent QI > 80%. Statistics for the LBF pressure are also included (gray lines) for reference. Also shown is the number of winds in each bin (right *y* axis). The cloud-layer depth is calculated as the difference between the pressures of the cloud top and the cloud base. The AMVs were binned in intervals of 20 hPa, with the first interval [0, 20] including AMVs with a one-level cloud layer and the last interval including AMVs with a layer deeper than 500 hPa.

RMSVD curve as layer depth increases is related to a tendency of the pMean to locate AMVs incorrectly in the vertical when layers are too deep and not to the intrinsic nature of deep-layer scenes. A similar analysis holds for VerAve.

2) COMPARISON OF HEIGHT ASSIGNMENTS FOR HIGH-LEVEL AMVS

Figure 8 further highlights the relationship among the model cloud top, the originally assigned pressure level, and the level of best fit, showing histograms of differences between these alternative pressure levels for single-layer ice clouds. The histograms show that the pressure assigned during the derivation (pAMV) tends to be lower than the model cloud top (pTop) for the tropics; that is, the AMVs tend to be placed too high in the vertical direction in relation to the model cloud top, whereas the opposite is the case for the extratropics. The histograms are consistent with the finding that assigning the AMVs to the originally assigned pressure or to the model cloud top gives broadly similar results for the extratropics (not shown).

In contrast, the LBF tends to be on average below the model cloud top in terms of height for the three geographical regions considered, with pLBF being, on average, 50 hPa larger than pTop (see right column of Fig. 8). Notice that the AMV height assignment does not play any role here, because both pTop and pLBF pressures are model-derived values. These results are consistent with the earlier finding that a height assignment lower in the atmosphere leads to better results (e.g., Figs. 1

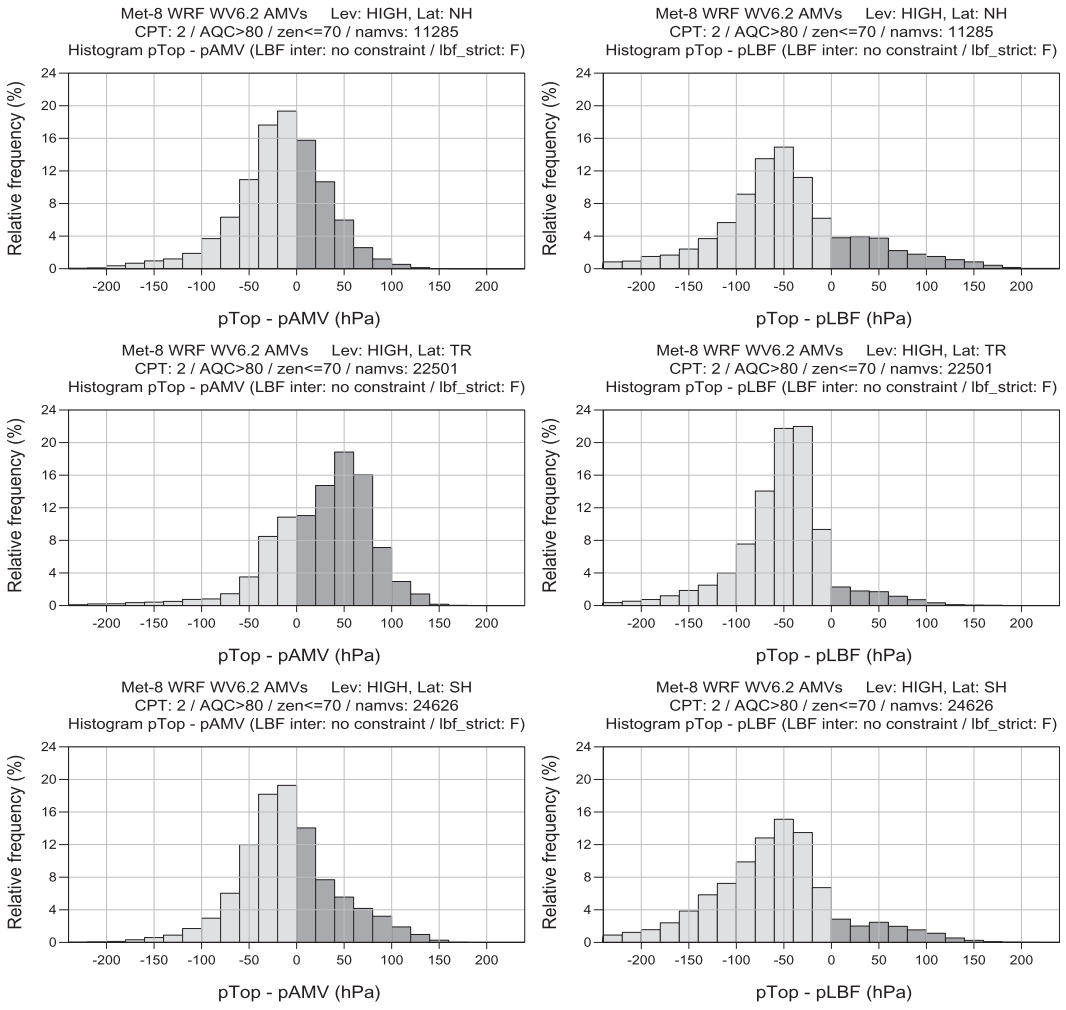

FIG. 8. Histograms of (left) pTop (pressure of the model cloud top) − pAMV (pressure assigned during the derivation) and (right) pTop − pLBF (pressure of the LBF) for WV6.2 AMVs in the Ice1 class, in the (top) NH (top), (middle) TR, and (bottom) SH.

and 5), and give further evidence to support the hypothesis that the best pressure to assign AMVs is not that of the cloud top, but a pressure within the cloud.

The two columns of Fig. 8 link the two aspects of AMV height assignment: 1) What is the most appropriate level for the assignment of AMVs? and 2) How should we estimate that level in height assignment algorithms? A simulation framework provides the true wind profile and a detailed description of cloud layers and therefore allows one to study separately how good the estimation of the cloud-top pressure is in a particular AMV dataset and whether the cloud-top pressure is the most representative level for AMVs.

3) LOW-LEVEL AMVS

We will now consider low-level AMVs. To simplify the interpretation, we again restrict the sample of AMVs to cases with one cloud layer only, this time to one liquid-water cloud layer (Liq1). Figures 9 and 10 show 2D histograms of speed and direction for low-level IR10.8 AMVs with a model-independent quality index QI > 80%. The figures show histograms for four types of model-equivalent winds: pAmvBcor, pBot, pMean, and VerAve. Table 4 shows summary statistics for the same AMVs and model-equivalent winds, and it also includes RMSVD and bias for pTop.

In comparing the results for the different interpretations of AMVs, one sees an improvement when the model equivalents for low-level AMVs are calculated either as a single level interpolated to a cloud-mean pressure (pMean) or as an average over the cloud layer (VerAve). In terms of RMSVD and the sharpness and symmetry of the distributions of speed and direction, both interpretations lead to overall better results than

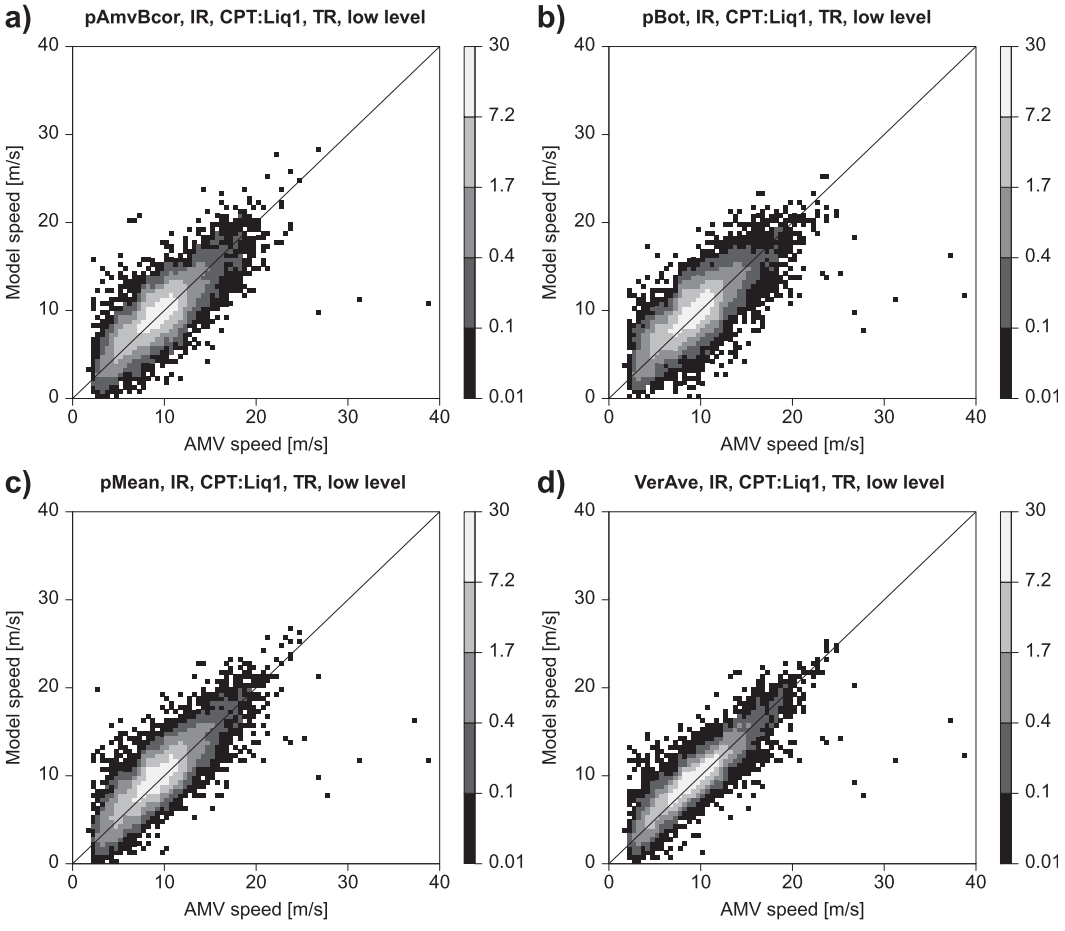

FIG. 9. Two-dimensional histograms of AMV and model speed as in Fig. 4, but for low-level IR10.8 AMVs in the tropics for which only one liquid cloud layer is present. Shown are results for the different AMV interpretations considered in this study: with the model wind linearly interpolated to (a) the bias-corrected pressure assigned to the AMV (pAmvBcor), (b) the bottom of the cloud (pBop), or (c) an average pressure over the cloud layer (pMean), or (d) with the model wind calculated as an average of wind over the cloud layer (VerAve).

pTop or pBot, and also pAmvBcor (see Figs. 9 and 10 and Table 4). Interpreting the AMVs as an average wind over the cloud layer (VerAve) gives the best results overall, with a clear advantage over the other model equivalents considered, including the pMean. Our ''capped'' variants of VerAve and pMean have also been considered but in the case of low-level winds do not yield a significant improvement (not shown).

There is no evidence from our statistics that low-level AMVs best represent the wind at the cloud base. Assigning the AMVs to the base of the cloud (*pBot*) or the top (*pTop*) gives similar results in terms of speed bias and RMSVD (e.g., Table 4), whereas assigning the wind to a level within the cloud (*pMean*) leads to overall the best comparisons for single-level interpretations of AMVs. In many derivation systems, low-level AMVs are considered to best represent wind at the cloud base, following work by Hasler et al. (1979), Le Marshall et al. (1993) and other considerations. According to our statistics, it appears that an average over the cloud layer may be more appropriate. It is worth noting here that height assignment to the cloud base is in any case difficult with the infrared imagery used and hence is subject to large uncertainties.

5. Conclusions

The main objective of the study described in this paper has been to improve understanding of the characteristics and origins of AMV errors and to guide developments in the use of AMVs in NWP, and it has approached the analysis of AMV errors by using a simulation framework. High-resolution model simulations provide a very sophisticated description of the atmosphere, including cloud variables, which allows one to explore alternative interpretations of the nature of AMVs.

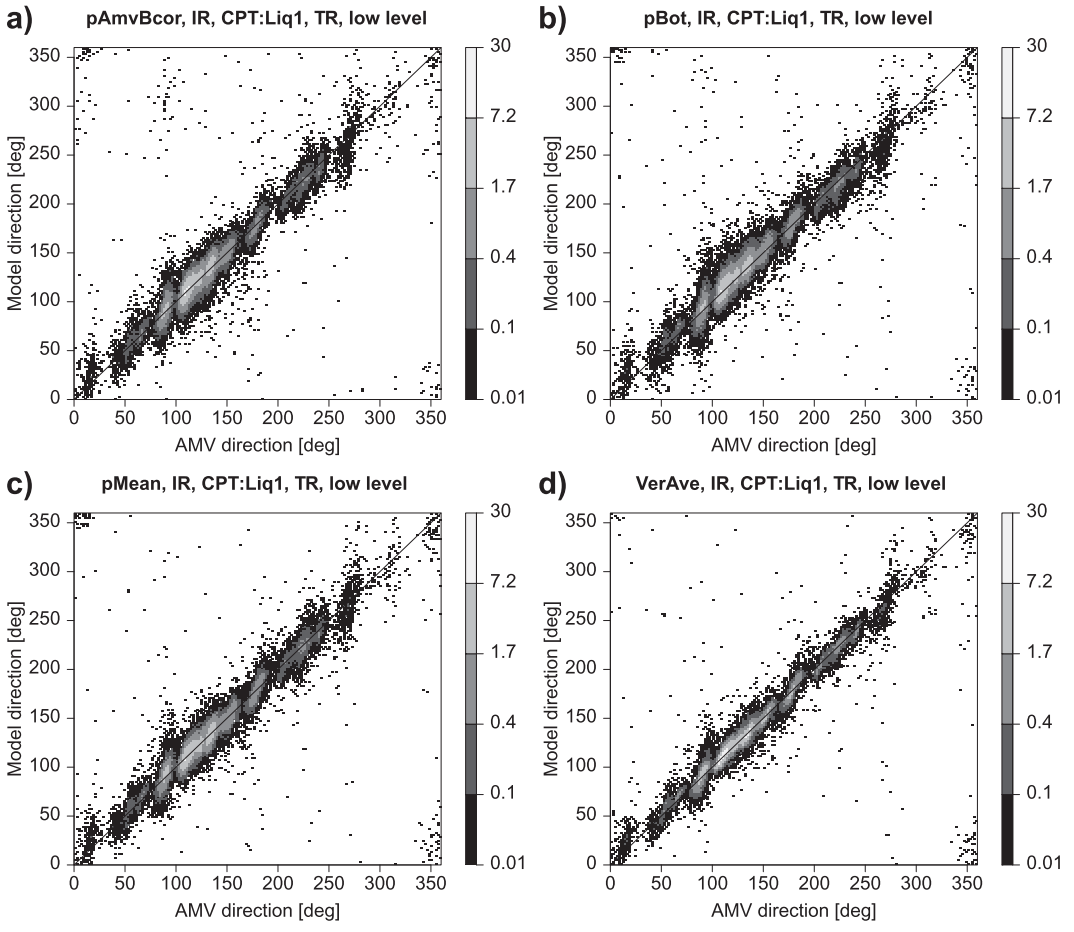

FIG. 10. As in Fig. 9, but for the direction of the AMV and model wind (‰ per 2° bin).

First, we presented evaluations of cloudy AMVs from WRF WV6.2 and IR10.8 simulated images, interpreted as horizontal and vertical averages. There were two main findings:

1) Horizontal and vertical averaging of the model wind consistently leads to better agreement between the AMVs and model-equivalent winds, with an improvement of up to ~5% for high-level AMVs and 20% for low-level AMVs. Vertical averaging gives more benefits in our study than horizontal averaging, with optimal layer depths of ~100–180 hPa.
2) Averaging over a layer not centered around the assigned pressure or interpreting the AMV as single-level observation at an adjusted pressure can have similar effects if, on average, the assigned pressure is significantly different from the most representative pressure level. In this case, the apparent improvement from layer averaging can be larger, but a significant portion can be achieved by interpreting the AMV as a single-level wind at an adjusted pressure level.

Second, we have presented and evaluated alternative interpretations of AMVs, related to the ambient cloud layer. The two main results from the AMV and model datasets used in the study are as follow:

1) For high-level AMVs and ice clouds, AMVs are more representative of the wind at a level within the tracked

TABLE 4. As in Table 3, but for low-level (pressure > 700 hPa) WRF IR10.8 AMVs in the Liq1 subset (QI > 80%).

		NH	TR	SH
No.		6116	61 731	24 132
AMV speed ($m\,s^{-1}$)		8.5	9.0	8.2
Speed bias ($m\,s^{-1}$)	pAmvBcor	−0.2	0.3	0.0
	pBot	−0.3	−0.5	−0.1
	pTop	−0.2	0.1	−0.1
	pMean	−0.2	−0.5	−0.3
	VerAve	−0.1	−0.4	−0.1
RMSVD ($m\,s^{-1}$)	pAmvBcor	2.3	2.2	2.4
	pBot	2.6	2.4	2.5
	pTop	2.5	2.7	2.8
	pMean	2.2	2.1	2.3
	VerAve	1.8	1.6	1.8

cloud, rather than the cloud top. Reassigning AMVs to a layer-average pressure or interpreting the AMV as representing an average wind over the cloud layer leads to clear improvements, provided that the cloud layer is not too deep. For deep layers, it appears beneficial to set a limit on the pressure increment or layer extent in relation to the cloud top.

2) For low-level AMVs and liquid-water clouds, the AMVs are more representative of a wind average over the cloud layer than of the wind at the cloud base or the cloud top. Reassigning AMVs to a layer-average pressure also brings improvements over the originally assigned pressure or the reassignment to the base or the top of the model cloud.

The above results have been obtained with a specific AMV derivation system, and further work is required to evaluate to what extent they are applicable to other AMV derivation systems and satellite instruments. Routine monitoring statistics produced at NWP centers show that established operational AMV datasets from different derivation systems share some characteristics (e.g., Cotton and Forsythe 2012), but it is also clear that there are considerable differences (e.g., Genkova et al. 2010). It would therefore be insightful to repeat this study using data from a different derivation system.

Our study finds some benefits from calculating AMV equivalents as layer and spatial averages, consistent with related findings of other authors (e.g., Velden and Bedka 2009; Weissmann et al. 2013). The findings provide some guidance on the design of an observation operator for AMVs in data assimilation in which AMVs are normally used as single-level point observations of wind. The optimal layer depths are likely to be situation dependent, and further research is needed in this respect. Note that the results presented here are likely influenced by the representativeness in the vertical direction of the wind field of the forecast model used. Results obtained with high-resolution radiosonde data may capture larger variability in the vertical dimension and therefore show a larger effect from averaging in the vertical direction. The results presented here in this respect are likely to be more indicative of the benefits to be expected in today's NWP systems, which will also not capture some finescale structures. Our results nevertheless suggest that treating AMVs as layer averages in NWP is likely to be beneficial in terms of improving comparisons between AMVs and short-range forecasts. The forecast impact of such a change depends on many other factors, such as the spreading of the observation information in the vertical direction through the assumed background error correlations and contributions from other observations, and these aspects will have to be assessed carefully.

Our study also finds that the positioning of the layer relative to the assigned pressure can have a marked effect on the behavior of the layer averaging, similar to results of Weissmann et al. (2013). Which positioning to choose, in turn, is related to how to interpret the pressure that is assigned to the AMV. The assigned pressure is currently interpreted by the users as a representative level for the provided wind estimate. If this estimate is not biased, layer-averaging centered around the assigned level seems the natural choice. If the assigned pressure level is a reliable estimate of the cloud top, averaging below this assigned pressure level is more justified. Further work is required to specify the situation-dependent extent and layer position for real data, for instance with the help of further cloud parameters such as cloud optical depth derived from the imagery.

When AMVs are interpreted as single-level wind observations, this study suggests that it is beneficial to assign AMVs to a representative level within the cloud rather than to an estimate of the cloud top for high-level AMVs or to an estimate of the cloud base for low-level AMVs. Further work is required to determine how this representative level can be derived in the absence of the detailed cloud information that is fully known in our simulation framework. It may be possible to derive such information from SEVIRI observations. Furthermore, our findings suggest that it may be beneficial either to use height assignments specifically designed for AMVs (rather than general cloud-top pressure products) or to develop height assignment corrections that are specifically designed to account for AMV characteristics (possibly derived on the user side). This aspect requires further discussion in the community; for practical reasons it may be best to continue to assign AMVs to the best available estimate of the cloud top but to develop corrections to the height assignment on the user side.

The detailed description of the true atmosphere provided by the simulation framework offers new avenues for progress both in AMV derivation and in data assimilation. Some examples regarding alternative views of what AMVs may represent have been shown in this paper, but there are other possibilities to explore, such as linking the layer averaging closer to the cloud type and cloud optical depth or the use of other filters for vertical averaging. The origins of the correlated errors could also be investigated further by using alternative AMV height interpretations as were used elsewhere in this study. The opportunities go beyond the analysis of AMVs; simulated imagery could be used, for example, to validate cloud classifications from observed imagery.

There are nevertheless limitations with the approach that should be studied further as well. Our study found significant height biases in our simulation; an analysis of their origin would require further investigations about the detailed performance of the height assignment algorithms, including further analysis of the representation of clouds in the model as well as of biases in the model fields, the radiative transfer, and the observations. Our experience highlights that a good characterization of the simulation itself is important to gauge to what extent results are applicable to real AMVs. There are also technical challenges: while high spatial model resolution and a longer study period are desirable, the computational cost and the volume of data set strong constraints on the simulations. Similar studies are currently being done by Lean et al. (2012).

Acknowledgments. The study was funded by EUMETSAT Contract EUM/CO/10/46000000785/RB. We express our thanks to Régis Borde for his support during the project and for producing the AMVs for the study, Hans-Joachim Lutz for the cloud analysis used in the AMV derivation, Steve Wanzong and CIMSS for providing the WRF simulation output, and Mary Forsythe and Tony McNally for their interesting comments and questions. The comments from three anonymous reviewers helped to significantly improve the manuscript.

REFERENCES

Borde, R., A. D. Smet, G. Dew, P. Watts, H.-J. Lutz, M. Carranza, and M. Doutriaux-Boucher, 2011: AMV extraction scheme for MTG-FCI at EUMETSAT. *Proc. 2011 EUMETSAT Meteorological Satellite Conf.,* Oslo, Norway, EUMETSAT, 10 pp. [Available online at http://www.eumetsat.int/groups/cps/documents/document/pdf_conf_p59_s1_09_borde_v.pdf.]

Bormann, N., G. Kelly, and J.-N. Thépaut, 2002: Characterising and correcting speed biases in atmospheric motion vectors within the ECMWF system. *Proc. Sixth Int. Winds Workshop,* Madison, WI, Int. Satellite Winds Working Group, 113–120. [Available online at http://www.researchgate.net/publication/228491110_Characterising_and_correcting_speed_biases_in_atmospheric_motion_vectors_within_the_ECMWF_system.]

——, A. Hernandez-Carrascal, R. Borde, H.-J. Lutz, and S. Wanzong, 2014: Atmospheric motion vectors from model simulations. Part I: Methods and characterization as single-level estimates of wind. *J. Appl. Meteor. Climatol.,* **53,** 47–64.

Büche, G., H. Karbstein, A. Kummer, and H. Fischer, 2006: Water vapor structure displacements from cloud-free Meteosat scenes and their interpretation for the wind field. *J. Appl. Meteor. Climatol.,* **45,** 556–575.

Cotton, J., and M. Forsythe, 2012: Fifth analysis of the data displayed on the NWP SAF AMV monitoring website. Met Office Rep. NWPSAF-MO-TR-027, 42 pp. [Available online at http://research.metoffice.gov.uk/research/interproj/nwpsaf/satwind_report/nwpsaf_mo_tr_027.pdf.]

Forsythe, M., J. Cotton, and R. Saunders, 2010: Improving AMV impact in NWP. *Proc. 10th Int. Winds Workshop,* Tokyo, Japan, Int. Satellite Winds Working Group, 8 pp. [Available online at http://www.eumetsat.int/website/home/News/ConferencesandEvents/DAT_2042632.html.]

Genkova, I., R. Borde, J. Schmetz, C. Velden, K. Holmlund, N. Bormann, and P. Bauer, 2010: Global atmospheric motion vector inter-comparison study. *Proc. 10th Int. Winds Workshop,* Tokyo, Japan, Int. Satellite Winds Working Group, 8 pp. [Available online at http://www.eumetsat.int/website/home/News/ConferencesandEvents/DAT_2042632.html.]

Hasler, A. F., W. C. Skillman, and W. E. Shenk, 1979: In situ aircraft verification of the quality of satellite cloud winds over oceanic regions. *J. Appl. Meteor.,* **18,** 1481–1489.

Lean, P., S. Migliorini, and G. Kelly, 2012: Studying the relationship between synthetic NWP-derived AMVs and model winds. *Proc. 11th Int. Winds Workshop,* Auckland, New Zealand, Int. Satellite Winds Working Group, 39 pp. [Available online at http://cimss.ssec.wisc.edu/iwwg/iww11/talks/Session5_Lean.pdf.]

Le Marshall, J., N. Pescod, A. Khaw, and G. Allen, 1993: The real-time generation and application of cloud-drift winds in the Australian region. *Aust. Meteor. Mag.,* **42,** 89–103.

Otkin, J. A., T. J. Greenwald, J. Sieglaff, and H.-L. Huang, 2009: Validation of a large-scale simulated brightness temperature dataset using SEVIRI satellite observations. *J. Appl. Meteor. Climatol.,* **48,** 1613–1626.

Rao, P. A., C. S. Velden, and S. A. Braun, 2002: The vertical error characteristics of GOES-derived winds: Description and experiments with numerical weather prediction. *J. Appl. Meteor.,* **41,** 253–271.

Rao, P. K., S. J. Holmes, R. K. Anderson, J. S. Winston, and P. E. Lehr, Eds., 1990: *Weather Satellites: Systems, Data, and Environmental Applications.* Amer. Meteor. Soc., 503 pp.

Saunders, R., and Coauthors, 2008: What can RTTOV-9 do for me? *Proc. 16th Int. TOVS Study Conf.,* Angra dos Reis, Int. ATOVS Working Group, 8 pp. [Available online at http://cimss.ssec.wisc.edu/itwg/itsc/itsc16/proceedings/3_2_Saunders.pdf.]

Velden, C. S., and K. M. Bedka, 2009: Identifying the uncertainty in determining satellite-derived atmospheric motion vector height attribution. *J. Appl. Meteor. Climatol.,* **48,** 450–463.

Weissmann, M., K. Folger, and H. Lange, 2013: Height correction of atmospheric motion vectors using airborne lidar observations. *J. Appl. Meteor. Climatol.,* **52,** 1868–1877.